Comparison of Indian summer monsoon rainfall anomalies in response to changes in snow depths and SSTs in a GCM

S. K. DASH, MANISH PALIWAL, S. K. PANDA* and SRINIVASARAO KARRI**

Centre for Atmospheric Sciences, Indian Institute of Technology Delhi, Hauz Khas, New Delhi – 110 016, India

**Department of Atmospheric Science, Central University of Rajasthan, Rajasthan – 305 817, India*

***Earth and Climate Science Area, National Remote Sensing Centre, Hyderabad, India*

e mail : skdash@cas.iitd.ac.in

सार – समुद्र सतह तापमान (SST), हिम अवारण/गहराई तथा मृदा नमी जैसी धीरे-धीरे बदलती सीमा की स्थितियों की भारतीय ग्रीष्मकालीन मॉनसून वर्षा (ISMR) परिवर्तिता में महत्वपूर्ण भूमिका है। इससे पहले के अध्ययनों में भारतीय ग्रीष्मकालीन मॉनसून वर्षा और समुद्र सतह तापमान विसंगतियों में अंतर-वार्षिक विविधताओं के बीच मजबूत संबंध दिखाया गया है। कुछ अध्ययनों से यूरेशियन महाद्वीप और भारतीय ग्रीष्मकालीन मॉनसून वर्षा (ISMR) पर सर्दियों/ वसंत ऋतु के बर्फ के बीच व्युत्क्रम संबंध का संकेत मिलता है। इस अध्ययन का उद्देश्य भारतीय ग्रीष्मकालीन मॉनसून परिसंचरण और संबद्ध वर्षा में एस एस टी और बर्फ की गहराई की विसंगतियों की सापेक्ष भूमिकाओं की जाँच करना है। वर्तमान अध्ययन में, 20 वर्षों की अवधि में एनसेम्बल मोड में संवेदनशीलता अध्ययन करने के लिए वर्णक्रमीय सामान्य परिसंचरण मॉडल का उपयोग किया गया है। समुद्र सतह तापमान और बर्फ की गहराई दोनों के प्रेक्षित तथा जलवायु संबंधी मूल्यों को अलग-अलग करके यहाँ चार प्रकार के संवेदनशील प्रयोग किए गए हैं। मॉडल सिम्युलेटेड ISMR अधिकांश मामलों में प्रेक्षित मानों से मेल खाते हैं जबकि आरंभिक स्थितियों में मॉडल को बर्फ की गहराई प्रदान की जाती है। चार प्रयोगों के परिणामों की परस्पर तुलना से पता चलता है कि प्रारंभिक बर्फ की गहराई के अभाव में मुख्य ग्रीष्मकालीन मॉनसून क्षेत्र में अनुकारी भारतीय ग्रीष्मकालीन मॉनसून परिसंचरण और इससे संबद्ध ISMR संबंधित प्रेक्षित क्षेत्र के करीब नहीं है यद्यपि इस मॉडल में प्रेक्षित किए गए समुद्र सतह तापमानों को सीमा शर्तों के अनुरूप दर्शाया गया है। जलवायु परिवर्तन के कारण भारतीय ग्रीष्मकालीन मॉनसून वर्षा में बर्फ की गहराई में उत्पन्न विसंगतियों के लिए मॉडल की प्रतिक्रिया जलवायविक हिम की उपस्थिति में समुद्र सतह तापमान की विसंगतियों के कारण अधिक है।

ABSTRACT. The slowly varying boundary conditions such as Sea Surface Temperature (SST), snow cover/depth and soil moisture have important roles to play in Indian Summer Monsoon Rainfall (ISMR) variability. Earlier studies have shown strong relationship between inter-annual variations in ISMR and SST anomalies. Some studies also indicate inverse relationship between the winter/spring snow over the Eurasian continent and the following ISMR. The objective of this study is to examine the relative roles of SST and snow depth anomalies in the Indian summer monsoon circulation and associated rainfall. In the present study, a spectral General Circulation Model has been used to conduct the sensitivity studies in the ensemble mode over a period of 20 years. Four types of sensitive experiments have been conducted here by varying the observed and climatological values of both SST and snow depth. Model simulated ISMR agrees well with the corresponding observed value in most of the cases where observed snow depths are provided to the model as initial conditions. Inter-comparison of the results of four experiments reveals that in the absence of initial snow depths, simulated Indian summer monsoon circulation and associated ISMR in the core monsoon region are not close to the respective observed fields even though observed SSTs are prescribed as boundary conditions to the model. The model response in terms of changes in ISMR to the snow depth anomalies in the presence of climatological SST is stronger than that due to SST anomalies in the presence of climatological snow.

Key words – Indian summer monsoon rainfall anomalies, Snow depth and sea surface temperature anomalies, Stream function and velocity potential.

1. Introduction

Indian summer monsoon is an annual weather event associated with high spatial and temporal rainfall variations and it affects the socio-economic conditions in India to a large extent. Regional rainfall variations affect agricultural productions, availability of drinking water and hydro-power, human health and similar other aspects of

the inhabitants. Therefore, near-to-correct prediction of rainfall amounts over different regions of the country during its summer monsoon season (June to September) is very important. It is well known that Indian Summer Monsoon Rainfall (ISMR) variability is partly controlled by the internal dynamics (Sperber and Palmer, 1996; Brankovic and Palmer, 2000; Krishnamurthy and Shukla, 2000; Goswami and Ajaya Mohan, 2001; Sperber, *et al.*, 2001; Cherchi and Navarra, 2003; Saha *et al.*, 2011) and partly by the slowly varying boundary conditions such as Sea Surface Temperature (SST), snow cover and soil moisture. Charney and Shukla (1981) had suggested that the Indian monsoon circulation is a dynamically stable system and its inter-annual variability is largely determined by slowly varying surface boundary conditions. Several earlier studies have demonstrated the strong relationship between inter-annual variability of ISMR and SST anomalies over the Pacific, Indian Ocean (including Arabian Sea) and the Atlantic (Shukla, 1975; Sikka, 1980; Keshavamurthy, 1982; Rao and Goswami, 1988; Krishna Kumar *et al.*, 1999; Clark *et al.*, 2000; Behera and Yamagata, 2001; Rajeevan *et al.*, 2002; Wang *et al.*, 2006; Kothawale *et al.*, 2008). A large number of studies have also been carried out to understand the relationship between the winter/spring season snow anomalies over the Eurasian continent and the following ISMR. Several studies (Hahn and Shukla, 1976; Shankar Rao *et al.*, 1996; Bamzai and Shukla, 1999; Kripalani and Kulkarni, 1999) based on observed snow data exhibit the inverse relationship between Indian summer monsoon and Eurasian and Tibetan snow depth anomalies. In their study, Dash *et al.* (2003 & 2005) analyzed the of characteristics of atmospheric circulations during contrasting years of high(low) winter/spring Eurasian snow depths based on observed data and identified some signals in the mid-latitude geopotential and velocity potential fields leading to deficient (excess) summer monsoon seasonal rainfall over India.

Sensitivity studies using General Circulation Models (GCMs) have also been conducted by several authors such as Barnett *et al.* (1989); Vernekar *et al.* (1995); etc. to study the impact of Eurasian and Tibetan snow anomalies on the Indian summer monsoon circulation and rainfall. Dash *et al.* (2006) in their study used a GCM to carry our sensitivity studies corresponding to contrasting summer monsoon cases and reaffirmed the negative relationship between Eurasian snow depth anomalies and ISMR. Turner and Slingo (2010) based on their ensemble integrations of HadAM3e demonstrated that snow forcing from the Himalaya region is dominant via a Blanford-type mechanism over the Tibetan Plateau leading to a reduced meridional tropospheric temperature gradient which eventually weakens the monsoon during early summer.

Although it is well known that both SST and snow anomalies play very important role in the simulation of Indian summer monsoon circulation and rainfall, the relative responses of a GCM to their changes is not known. Model simulated ISMR is close to its observed value when observed snow and SST are used in the model integrations and hence today the observed boundary conditions are used in any model experiment. It will be interesting to use both climatological and observed SST and snow and design experiments to examine the relative roles of SST and snow depth anomalies in affecting the Indian summer monsoon circulation and associated rainfall.

2. The model and datasets

In the present study, the IITD spectral GCM has been used to conduct sensitivity studies to examine the relative roles of SST and Eurasian snow depth in simulating the Indian summer monsoon. This T80L18 model is of horizontal resolution T80 in the triangular truncation (equivalent to $1.4° \times 1.4°$ grid) and it has 18 sigma levels in the vertical. The details of the spectral GCM are available in Dash and Chakrapani (1989). This model with T80 resolution has been successfully used by Dash *et al.* (2006) in demonstrating the role of spring time excess Eurasian snow depth anomaly in reducing the following ISMR.

The original version of the model belonged to the European Centre for Medium Range Weather Forecasts (ECMWF) at horizontal resolution T21L10. Earlier, the T21 model was successfully used for simulating circulation patterns over India (Dash and Chakrapani, 1989). This model is based on the spectral representations of nonlinear-coupled equations for momentum, thermodynamics, moisture, continuity and the hydrostatic relation. In practice, the model equations contain the spherical harmonics of vorticity, divergence, moisture and temperature at 18 vertical sigma levels and logarithm of surface pressure. The conventional finite difference scheme in sigma coordinates is used for the vertical discretization. The semi-implicit scheme is used for time integration. The details of the physics packages used in this study are given in Dash and Chakrapani (1989).

Weekly values of Reynolds-observed SSTs (Reynolds and Smith, 1994) are interpolated into their daily values which are used as the lower boundary condition for the model integration. Climatological daily SST are obtained from the Reynolds-OI SST. Daily observed values of snow have been obtained from NCEP/NCAR reanalysis and snow climatology is prepared using 20 years observed data. All other required surface boundary parameters and six hourly (0000, 0600,

1200 and 1800 UTC) values of temperature, *u* and *v* winds, specific humidity and surface pressure are obtained from the National Center for Environmental Prediction/National Centre for Atmospheric Research (NCEP/NCAR) reanalyzed dataset at 2.5° × 2.5° resolution (Kalnay *et al.*, 1996). These initial values are used in the model integrations after their due conversion into the model required input format.

Model integrated daily rainfall ate used to compute the seasonal mean (JJAS) precipitation values and these are examined to evaluate the model performance in simulating the normal, deficit and excess monsoon years as per the definition of the India Meteorological Department (IMD). Validation of model simulated rainfall has been done using moderate to high resolution datasets, such as IMD gridded rainfall (Rajeevan *et al.*, 2005) and Global Precipitation Climatology Project (GPCP) at 1° × 1° resolutions and those of Asian Precipitation - Highly Resolved Observational Data Integration Towards Evaluation of the Water Resources (APHRODITE) and Climate Research Unit (CRU) at 0.5° × 0.5° resolutions. The model simulated rainfall have been interpolated to the corresponding resolutions of the data sets for inter-comparison purpose. For validation of model circulation such as the upper and lower level winds, stream functions and velocity potentials, NCEP/NCAR reanalysis dataset at 2.5° × 2.5° resolution has been used.

3. Integration of model and experimental design

As stated earlier, in this study, IITD spectral GCM at T80L18 resolution has been integrated in the ensemble mode for a period of 20 years from 1985 to 2004 to generate daily model climatological fields. Each model integration is completed up to the end of September using daily climatological/observed SST values and initial climatological/observed snow depths. In this study, eleven member ensemble seasonal integrations have been made with initial conditions of 25th April to 5th May in each of the 20 years from 1985 to 2004. Daily output fields such as wind, temperature, moisture and geopotential at 18 vertical sigma levels have been saved along with surface pressure and accumulated rainfall for further analysis.

Four types of sensitivity experiments have been conducted by varying the observed and climatological values of SST and snow depths for the entire period of integration with a view to examine their relative roles in Indian summer monsoon simulations. In Exp-1, climatological SST and snow are used as surface boundary conditions. Climatological snow is replaced by observed snow in Exp-2 to study the impact of observed snow in inter-annual variability of summer monsoon over India. Exp-3 is based on the observed SST and climatological

snow. Both observed SST and snow are used in Exp-4 to examine their relative roles in the inter-annual variation of ISMR and circulation patterns.

4. Model simulated Indian summer monsoon climatology

Indian summer monsoon is manifested by the semi-permanent circulation features such as heat low, monsoon trough, cross-equatorial low level westerly jet over the Arabian Sea, Tibetan anticyclone and the upper level tropical easterly jet to its south. In this section we discuss the lower and upper level circulation features represented by 850 and 200 hPa wind fields. The most important parameters of Indian summer monsoon are the climatology of the rainfall for the monsoon season (JJAS) as a whole as well as the monthly mean rainfall amounts in June to September. The quantum of rainfall over the Indian landmass and its spatial distribution in millimeters per day are computed and compared with the corresponding fields obtained from various other data sources as discussed in the earlier section.

4.1 *Seasonal rainfall*

Figs. 1(a-d) shows the difference of ensemble mean (based on 11 members) of model simulated JJAS rainfall over Indian landmass from the corresponding IMD mean rainfall for the period of 20 years (1985-2004) in all the four experiments. Figs. 1(a-d) indicate positive biases in model simulated rainfall over the western region of India compared to that of IMD. Thus the model overestimates JJAS mean rainfall over the Western Ghats and parts of Maharashtra and Karnataka in all the four experiments. This positive model bias is about 5-10 mm/day as against IMD values. On the other hand, there is an underestimation of simulated rainfall of about 5 mm/day in the foothills of the Himalayas. Such overestimation and underestimation of the model rainfall might have happened due to associated Gibbs bias of spectral fitting (Dash and Mohandas, 2005) which does not resolve the orography correctly over Indian monsoon region. Close examination of Figs. 1(b&d) indicates close to zero bias as against IMD values over a large part of central India as compared to that in Figs. 1(a&c). Such improvements in the rainfall simulation in central India may be attributed to the use of observed snow in Exp-2 and Exp-4. Again the areal coverage of less rainfall in the Himalayan foothills, especially in the northeast India is less in Exp-2 and Exp-4 as compared to those in Exp-1 and Exp-3.

The model rainfall is also validated against 0.5° × 0.5° APHRODITE rainfall for the Indian region. Figs. 2(a-d) show the difference of ensemble average (based on 11 members) of model simulated seasonal
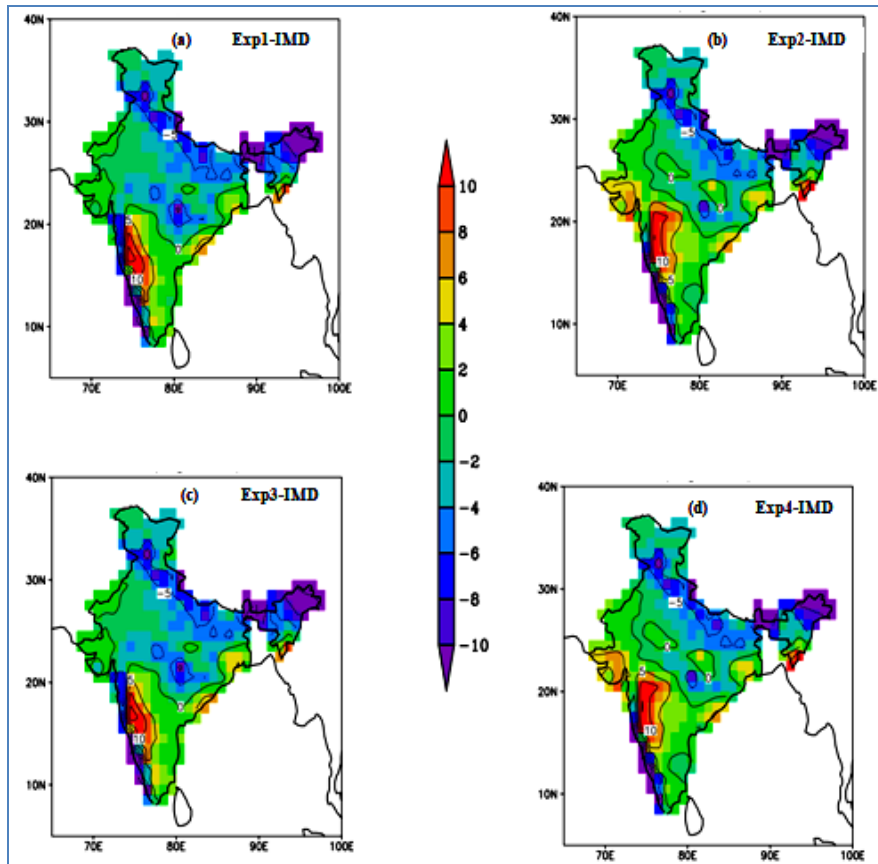
Figs. 1(a-d). Differences of ensemble mean (11 members) of model simulated seasonal (JJAS) rainfall of 20 years (1985-2004) from respective IMD rainfall (mm/day) for (a) Exp-1, (b) Exp-2, (c) Exp-3 and (d) Exp-4

rainfall over India for the 20 years period (1985-2004) in all the four experiments from the corresponding APHRODITE mean rainfall. The bias patterns in Figs. 2(a-d) are almost similar to those in Figs. 1(a-d) although there are variations in intensity. The model simulated rainfall in all the four experiments are closer to APHRODITE rainfall than to IMD gridded values. The area of coverage of the least bias in the range of -2 to +2 mm/day in the simulated rainfall, especially in the central India, as seen in Figs. 2(b&d) suggests that the observed snow prescribed in Exp-2 and Exp-4 might have helped in simulating closer to observed rainfall as compared to those in Exp-1 and Exp-3.

In order to confirm the effect of observed snow on the simulated precipitation, we have chosen another set of 0.5° × 0.5° rainfall data from CRU. Figs. 3(a-d) depicts the difference of 11 members ensemble mean of model simulated JJAS rainfall over India for the period of 20 years (1985-2004) in all the four experiments from the corresponding CRU mean rainfall. Detailed comparison of Figs. (1-3) indicates that at the regional scale, there are

some differences in the precipitation biases over the Western Ghats, the Himalayas and the northeast India against the three sets of rainfall data. Nevertheless, the rainfall biases in the central are similar in all the three datasets. More or less, the precipitation simulated with observed snow as surface boundary conditions in Exp-2 and Exp-4 brings out the JJAS rainfall closer to IMD gridded, CRU and APHRODITE rainfall values in certain parts of India, especially over the central India. After comparing with the above three different data sources we can infer that the observed snow plays an important role in the spatial distribution of rainfall over the Indian region.

4.2. *850 hPa wind*

In this section we have analyzed the model simulated seasonal winds in the lower atmosphere. Figs. 4(a-d) shows the difference of ensemble mean of lower level winds at 850 hPa simulated by the model for JJAS in all the four experiments from the corresponding values in NCEP/NCAR reanalysis. In the absence of observed winds, here NCEP/NCAR wind is used for inter-comparison.
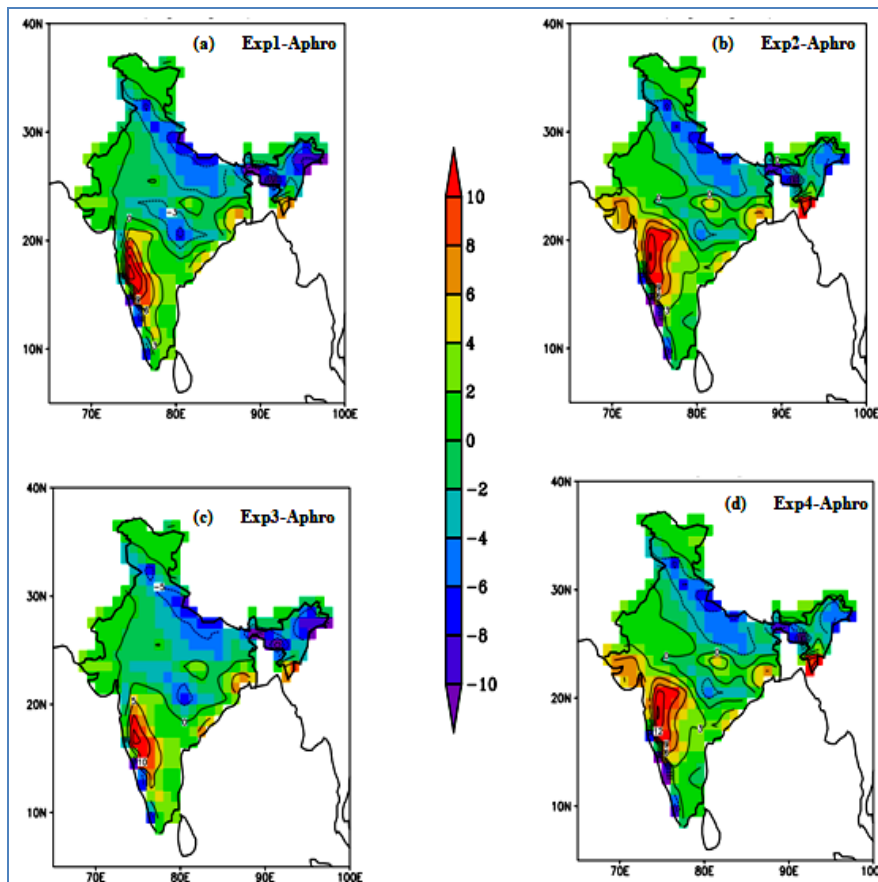
Figs. 2(a-d). Differences of ensemble mean (11 members) of model simulated seasonal (JJAS) rainfall (mm/day) of 20 years (1985-2004) from respective APHRODITE rainfall (mm/day) for (a) Exp-1, (b) Exp-2, (c) Exp-3 and (d) Exp-4

The difference fields in Figs. 4(a-d) show that the model overestimates lower level winds over the peninsular India and the Himalayas in all the four experiments. However, in case of the observed snow as surface boundary conditions [Figs. 4(b&d)], the positive biases over the Himalayas have much reduced in comparison to those in Figs. 4(a&c). Over central India, the wind biases are close to zero and in the range of -2 to +2 m/sec in Figs. 4(b&d) when observed snow are provided to the model. Over the same region, the wind biases are more by -2 m/sec in case of climatological snow as initial surface conditions.

Figs. 4(a&c) representing Exp-1 and Exp-3 shows weaker winds as compared to the observed values over central Indian region while the areal extent of the weaker winds is very less in Exp-2 and Exp-4 as seen in Figs. 4(b&d). This reduced weakness in the strength of wind might have happened because of the observed snow prescribed in Exp-2 and Exp-4. The other major difference among the four experiments is noted over the Himalayan region which confirms the role played by the observed snow in low level circulation. In Figs. 4(b&d) the difference in wind from the observed values over this region is very less (0-2 m/s) while on the other hand the difference is noticeably large (6-8 m/s) in Figs. 4(a&c). Thus after a close examination, it is inferred that the prescription of observed snow in the model plays a significant role in simulating lower level monsoon circulation.

4.3. *200 hPa wind*

Figs. 5(a-d) depicts the differences of ensemble mean of upper level wind (200 hPa) simulated by the model for the season (JJAS) as a whole for all the four experiments from the corresponding upper level values from NCEP/NCAR reanalysis. Figs. 5(a&c) representing Exp-1 and Exp-3 shows weaker winds as compared to the observed values over south and central Indian region mostly by 4-6 m/sec and even by 6-8 m/sec over the north Bay of Bengal. In Figs. 5(b&d), where observed snow has
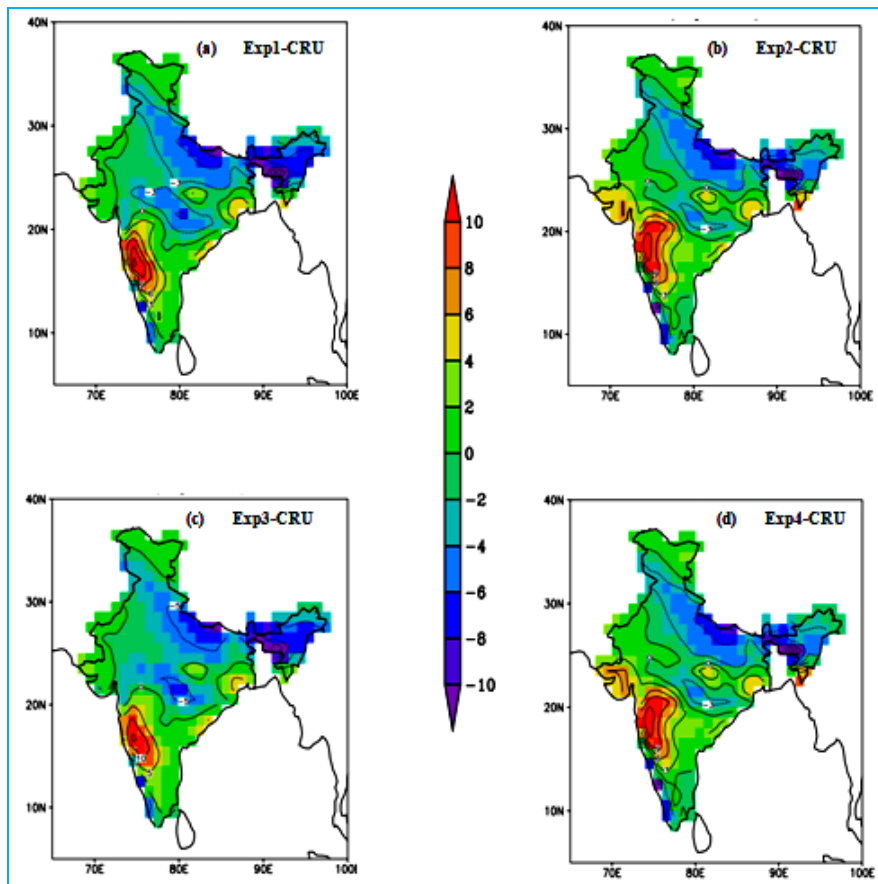
Figs. 3(a-d). Differences of ensemble mean (11 members) of model simulated seasonal (JJAS) rainfall (MM/day) of 20 years (1985-2004) from respective CRU rainfall (mm/day) for (a) Exp-1, (b) Exp-2, (c) Exp-3 and (d) Exp-4

replaced the climatological snow in the model, the biases in the upper level winds have reduced considerably to 0-2 m/sec over the same south and central Indian region. In the north India, there are considerable wind biases (up to 6 m/sec) in Figs. 5(a&c) which have been almost reduced to 0-2 m/sec in the presence of observed snow in Figs. 5(b&d). Over the Himalayas, the wind biases have changed from positive to negative when observed snow replaces climatological snow in the model experiments 2&4. Comparison of Figs. 5(a&c) with Figs. 5(b&d) definitely indicates the sensitivity of the upper level model winds to the observed Himalayan snow, but the reversal of phase in wind biases could have been due to the inaccuracy of snow depths and covers as estimated and prescribed to the model experiments. There could be over-estimation of the observed snow. On the whole, after a close examination, it is inferred that the prescription of observed snow in the model plays a significant role in simulating lower level monsoon circulation.

4.4. *Characteristics of velocity potential*

The velocity potential field is an useful parameter which reveals the circulation characteristics to a large extent. Figs. 6(a-c) illustrates the difference in the JJAS mean velocity potential between Exp-4 and other experiments at 200 hPa. In Fig. 6(a), the negative values show the large scale upper level divergence over East Asia and the positive values indicate the convergence over Eastern/Central Pacific. This figure exhibits the difference between results obtained from the combined effect of observed SST and snow on one hand and that of climatological SST and snow on the other. It suggests the impact of observed SST and snow in simulating stronger divergence at the upper level in the summer monsoon region. Fig. 6(b) shows the difference between velocity potential fields due to the combined effect of observed SST and snow in Exp-4 and that of climatological SST and observed snow in Exp-2. Almost no difference in velocity potential in Fig. 6(b) suggests the negligible impact of replacing climatological
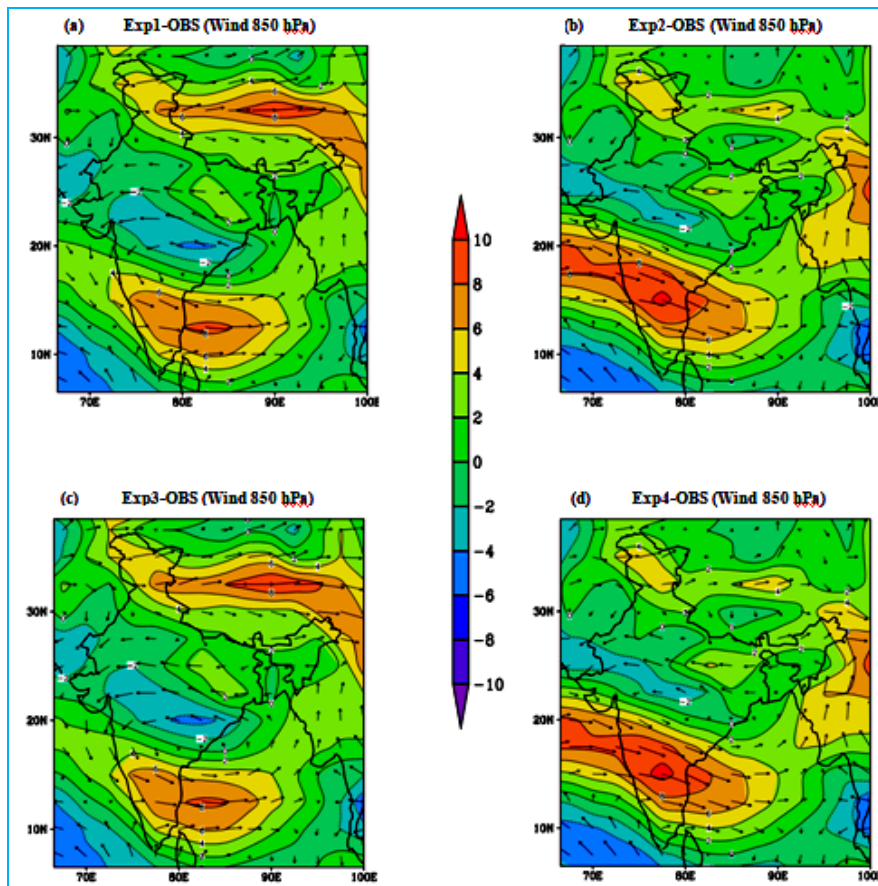
Figs. 4(a-d). Differences of ensemble mean (11 members) 850 hPa JJAS wind (m/sec) from corresponding NCEP/NCAR reanalysis

SST values by their observed ones as boundary condition in the experiments. Similarly, Fig. 6(c) shows the impact of observed snow in the form of stronger upper level divergence field over East Asia. Figs. 6(a&c) are broadly similar with very little difference between them, that is, the convergence and divergence fields are stronger due to the effect of observed snow. On the other hand Fig. 6(b) shows the least difference between Exp-4 and Exp-2, where observed snow is used.

Examination of divergence/convergence centres in the velocity potential difference fields at the lower level in Figs. 7(a-c) indicates corresponding convergence/divergence centers in Figs. 6(a-c). As in case of the upper level velocity potential anomaly fields, the lower level anomaly fields also bring out the dominant impact of replacing the climatological snow by the observed snow values as compared to replacing climatological SST by observed SSTs in the model experiments.

4.5. *Characteristics of stream function*

Stream function is another parameter which needs to be examined in the context of circulation. Stream function differences at upper and lower levels are shown in Figs. (8&9) respectively. Fig. 8(a) shows the difference between the upper level stream functions simulated in Exp-4 and Exp-1 respectively. Similarly Fig. 8(b) depicts the stream function difference fields between Exp-4 and Exp-2 and Fig. 8(c) those between Exp-4 and Exp-3. In Exp-4 both SST and snow values provided to the model are the observed ones whereas in Exp-1 and Exp-3 climatological snow values are used as initial conditions along with climatological and observed SSTs respectively as surface boundary conditions in the model. In Exp-2, SSTs provided to the model are their climatological values. Thus, Fig. 8(a) shows the relative influence of observed SST and snow with respect to climatological SST and snow. On the other hand, Fig. 8(b) indicates the relative impact of observed SST with respect to that of the climatological SST on the upper level stream function.
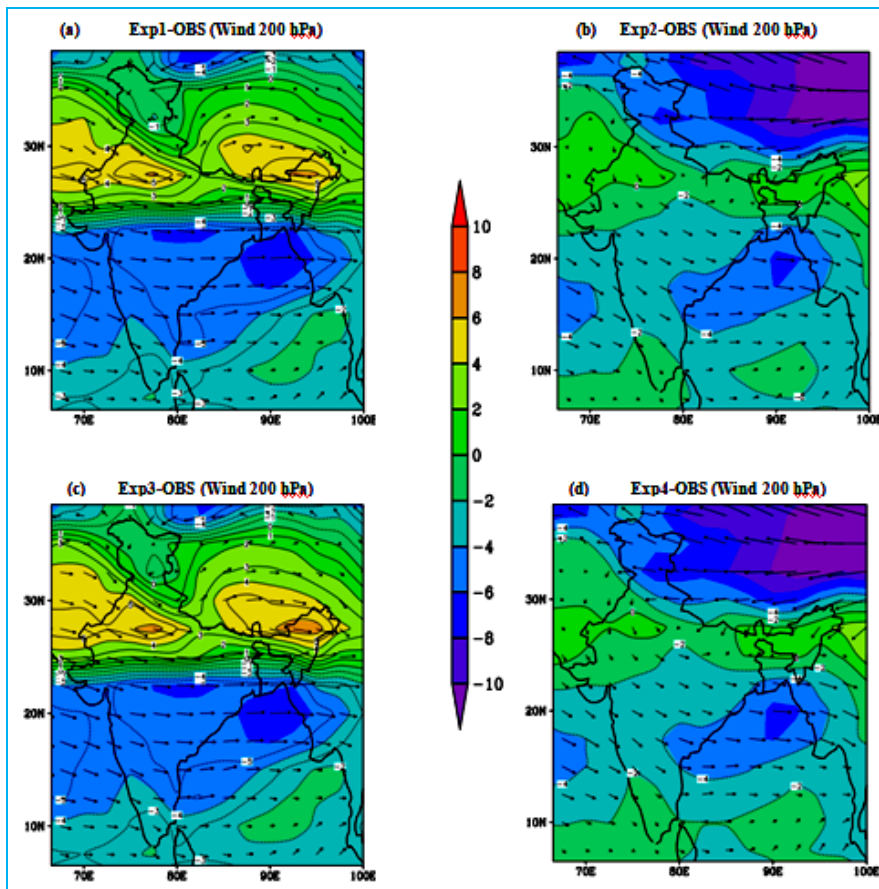
Figs. 5(a-d). Differences of ensemble mean (11 members) 200 hPa JJAS wind (m/sec) from corresponding NCEP/NCAR reanalysis
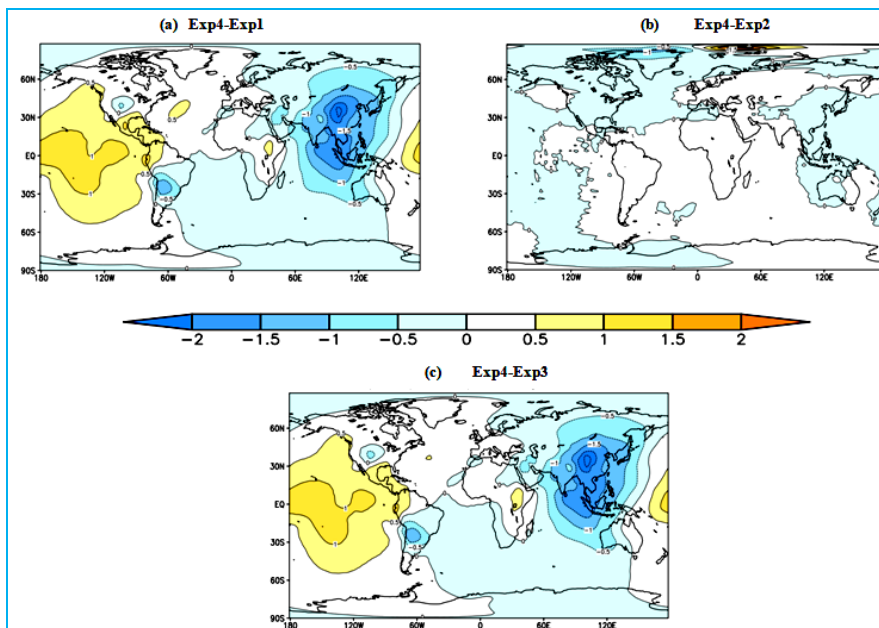
Figs. 6(a-c). Model simulated ensemble mean (11 members) seasonal (JJAS) Velocity Potential difference fields at 200 hPa (a) Exp4-Exp1, (b) Exp4-Exp2 and (c) Exp4-Exp3
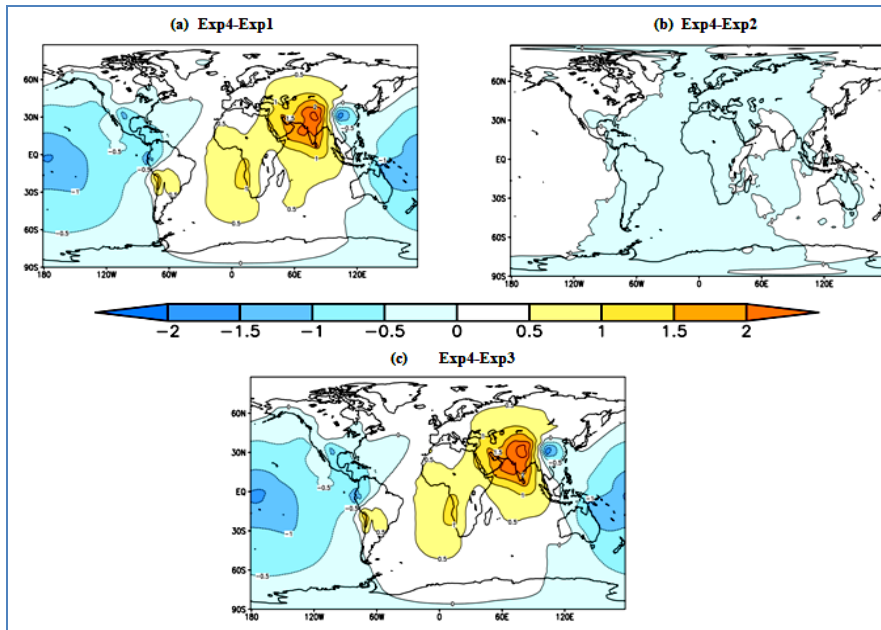
Figs. 7(a-c). Model simulated ensemble mean (11 members) seasonal (JJAS) Velocity Potential difference fields at 850 hPa (a) Exp4-Exp1, (b) Exp4-Exp2 and (c) Exp4-Exp3
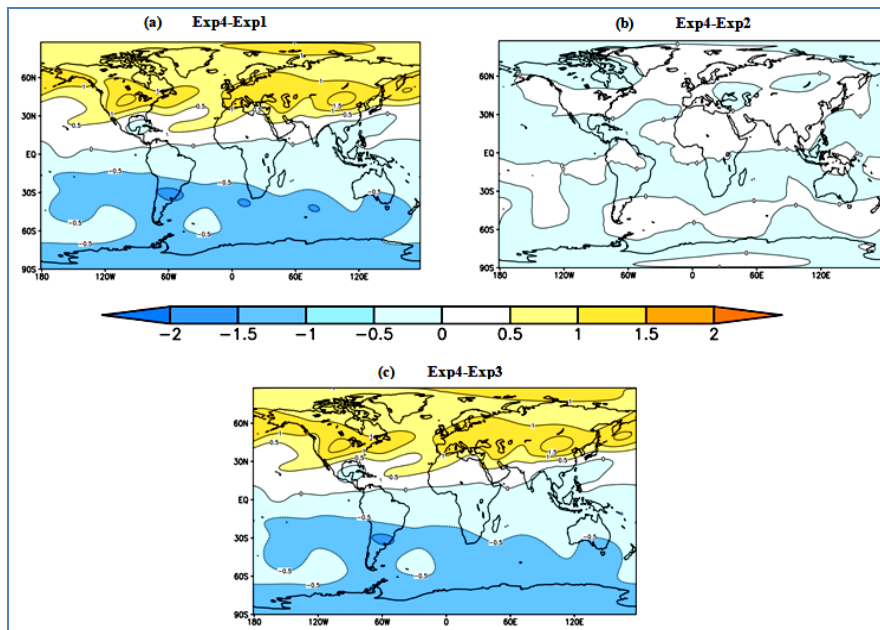
Figs. 8(a-c). Model simulated ensemble mean (11 members) seasonal (JJAS) Stream Function difference fields at 200 hPa (a) Exp4-Exp1, (b) Exp4-Exp2 and (c) Exp4-Exp3

Similarly, Fig. 8(c) indicates the relative impact of observed snow with respect to that of the climatological snow on the upper level stream function. The patterns of 850 hPa stream function for Exp-4 and Exp-2 are broadly in agreement with each other and hence Fig. 9(b) shows the least difference field. Since in both Exp-4 and Exp-2 observed SST was prescribed to the model, Fig. 9(b) reveals the negligible impact of observed SST on the lower level stream function. Comparative examination of Figs. 8(a-c) reveals results similar to those obtained in
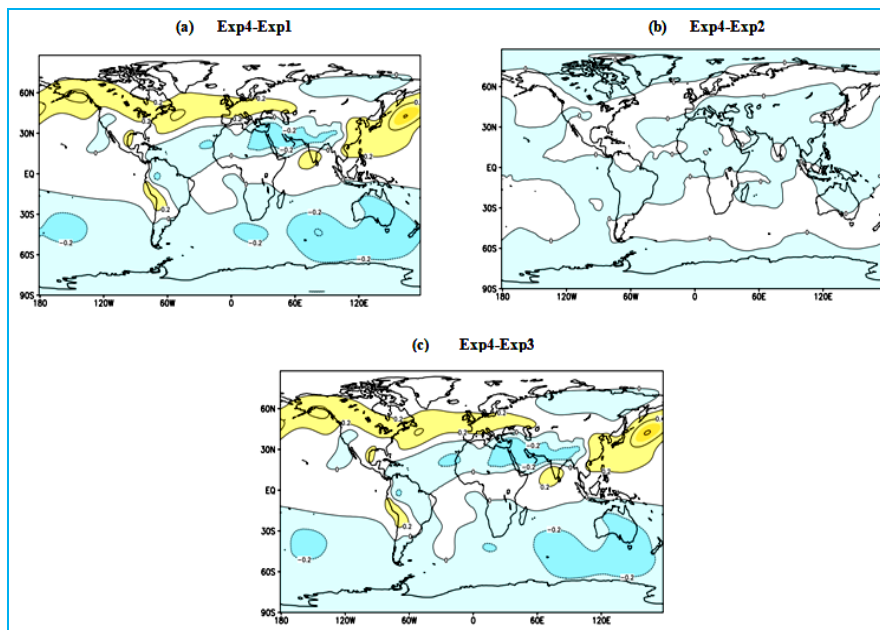
Figs. 9(a-c). Model simulated ensemble mean (11 members) seasonal (JJAS) Stream Function difference fields at 850 hPa (a) Exp4-Exp1, (b) Exp4-Exp2 and (c) Exp4-Exp3

case of earlier circulation parameters, *i.e.*, prescription of observed snow in the model has more impact on the upper level stream function as compared to that of observed SST. Comparative examination of Figs. 9(a-c) reveals result similar to that at 850 hPa. Thus it is inferred that circulation at both the lower and upper levels of the atmosphere are more sensitive to the prescription of observed snow to the model as compared to the observed SST.

5.   Inter-annual variations in ISMR

In order to examine the relationship between inter-annual variation of snow, SST and ISMR, first we have identified weak and strong snowfall years over western Eurasia as done in Dash *et al.* (2005). Western Eurasia region covering (25° E-70° E and 35° N-65° N) has been identified and the average of NCEP/NCAR reanalyzed daily snow depth values over this region has been calculated. Their mean values for the months of December, January and February (DJF) are computed and from those values the mean of the series and the standard deviations are calculated over Eurasian region for the years 1985-2004. The standardized snow depth anomaly of each year for the period 1985-2004 is obtained by dividing the departure of each year from the normal by the standard deviation. The years having snow depth anomaly between ±0.5 standard deviations are considered as normal snow depth years. Similarly, the years having snow depth anomaly equal to or above +0.5 standard

deviation are taken as high snow depth years and those having equal to or less than -0.5 standard deviation snow depth anomaly are identified as low snow depth years as mentioned in Dash *et al.* (2005). Based on UCAR data (1985-2004), SST anomalies have also been calculated over the Nino 3.4 region (5° N-5° S and 170° W-120° E). Using the their standard deviations, years have been categorized as El Nino (standard deviation equal or above +1), Normal (±1 standard deviation) and La Nina (with standard deviation -1 or less). In the similar way, ISMR anomalies based on IMD rainfall values have been computed and the years having ISMR anomaly more than or equal to +1 standard deviation are termed as excess monsoon years and those less than or equal to -1 standard deviation are considered as deficient monsoon years. The rest of the years are categorized as normal monsoon years. Based on the above criteria, classification of years with different categories of observed snow, SST and ISMR and also with model simulated ISMR in Exp-4 has been done in Table 1.

Results in Table 1 can be understood in the following way. In all the years 1990, 1991, 1992, 1993, 1995 and 1996 of normal (N) snow and normal SST, the ISMR was observed to be either normal or excess (E). Similarly, in the years 1985, 1988 and 2000 when there were normal snow and low (L) SST, the observed ISMR was either normal as in 1985 and 2000 or excess as in 1988. Further, during normal SST and low snow (2001, 2003 and 2004) ISMR was normal. Thus, when either

TABLE 1

**Classification of (UCAR) Nino 3.4 region SST, snow depth NCEP/
NCAR reanalysis-2), observed (IMD) Indian summer monsoon
rainfall (ISMR) and model simulated ISMR in Exp-4
for the period 1985-2004
(Here N, D and E stand for Normal, Deficient and Excess
ISMR respectively. Similarly N, L, H stand for Normal,
Lowand High SST &snow depth respectively)**

Year	SNOW	SST	Observed ISMR	Exp-4 ISMR
1985	N	L	N	N
1986	H	N	D	N
1987	N	H	D	D
1988	N	L	E	N
1989	H	L	N	N
1990	N	N	E	N
1991	N	N	N	N
1992	N	N	N	N
1993	N	N	N	N
1994	H	N	E	E
1995	N	N	N	N
1996	N	N	N	D
1997	H	H	N	N
1998	H	N	E	E
1999	L	L	N	E
2000	N	L	N	N
2001	L	N	N	N
2002	L	N	D	N
2003	L	N	N	N
2004	L	N	N	N

snow or SST was normal and the other was low, the ISMR was observed to be normal in most of the years and excess only in one year 1988. In 1989, the effects of high snow and low SST might have been neutralized to lead to normal ISMR. In 1999, low snow and low SST gave rise to normal ISMR although model simulated excess rain. On the other hand when either snow or observed SST was normal and the other surface boundary condition was high (H) there were either deficient (1986 and 1987) ISMR or excess (1994 and 1998). The excess rainfall in 1994 and 1998 seems to be in contradiction to its accepted inverse relationship with snow and SST. Again in 1997, in spite of both the surface conditions being high, ISMR was normal.

While validating model simulated ISMR, it is found to agree with observation in 14 years out of 20 years of study. In three more years (1988, 1990 and 1999) when the model simulated ISMR is normal, the observed value

is excess and *vice-a-versa*. Similarly in another three years (1986, 1996 and 2002) when ISMR in Exp-4 is normal, the observed value is deficient and *vice-a-versa*.

In Table 1, we notice three abnormal years 1994, 1997 and 1998 during which despite having high snow and/or high SST, ISMR is either normal or excess both in IMD observed and model simulations. In order to understand the anomalies in these years, we examine the circulation at 850 hPa since the low level wind represents the rainfall intensity to a large extent as shown in Figs. 10(a-c). In the years 1994 and 1998, in spite of adverse snow and/or SST, the low level jet is stronger which might be the reason behind the excess rainfall in these years. In 1997, the circulation is less in strength which might have contributed to deficient and normal rainfall. Similarly, 2002 is another abnormal year when there was deficient ISMR in spite of low observed snow and normal observed SST. In this year the model in Exp-4 simulates normal ISMR.

The inter-annual variations in rainfall as observed in IMD data and simulated in the four model experiments are shown in Fig. 11. Comparative study indicates that Exp-1 and Exp-3 simulate less rainfall than observed in almost all the years. On the other hand, simulated rainfall in Exp-2 and Exp-4 are closer to the respective observed values. These results signify the well known fact that the observed values of SST largely influence model performance in simulating rainfall closer to its observed values. Closer examination of rainfall amount in Fig. 11 indicates that Exp-4 performs much better than Exp-2. Out of 20 years of study, 14 years have shown good proximity to the observed rainfall in case of Exp-4. Moreover, in 1985, 1989, 1992, 1996, 1997, 1998 and 2003 the model simulated JJAS rainfall equals or almost equals the corresponding observed values. This clearly demonstrates the model sensitivity to observed SST and snow.

Fig. 12 shows the inter-annual JJAS rainfall anomalies as simulated in all the four experiments from the corresponding IMD values. As shown in the figure, Exp-4 simulated rainfall is closer to that of IMD in most of the years. For example in 14 years out of total 20 years of model simulation, the rainfall anomalies in Exp-4 are within the range of ±0.5 whereas in 9 years there is almost no difference between the simulated JJAS rainfall and the corresponding IMD value. Only in 5 years, there are rainfall differences more than or equal to ±1.

6.   Model sensitivity towards SST and snow combination

The magnitudes of ensemble mean (11 members) model simulated JJAS rainfall in each of the 20 years
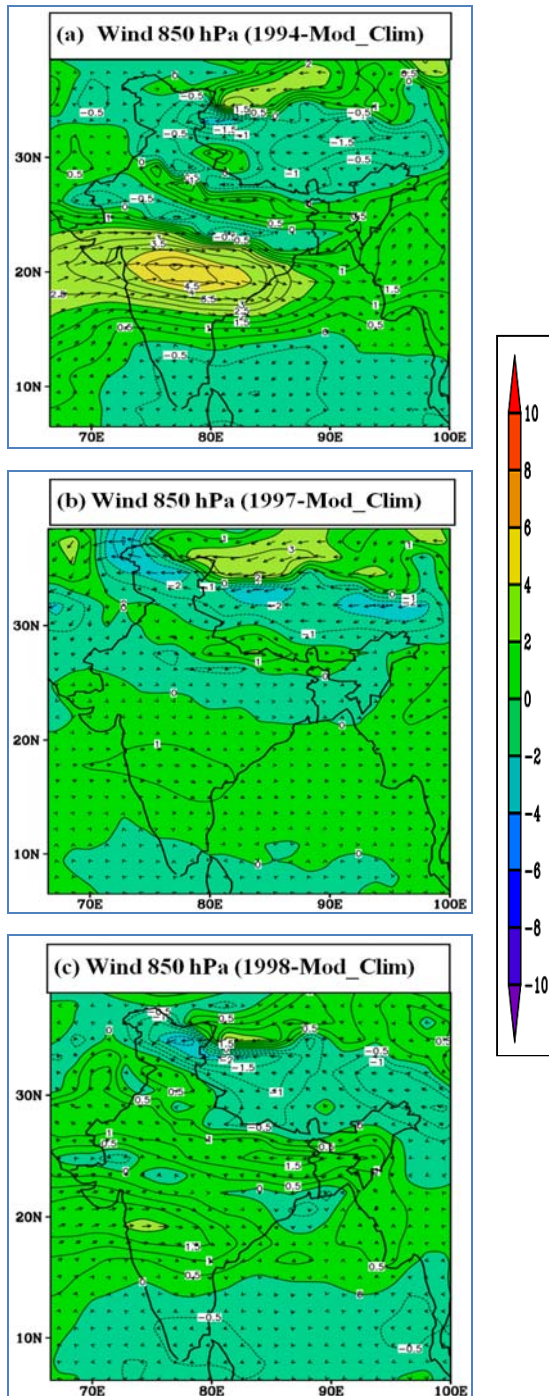
Figs. 10 (a-c). Model simulated wind anomalies (m/s) at 850 hPa with respect to ensemble mean in the years 1994, 1997 and 1998

(1985-2004) have been calculated in all the four experiments and compared with the respective IMD values. The inter-annual variations are represented in terms of box-and-whisker plots as shown in Fig. 13. Each

box plot is a non-parametric statistical summary of 20 years of rainfall. Each plot shows the median (the horizontal line in each box), the lower and upper quartiles (the lower and upper edges of the box) and the spread represented by minimum and maximum values (the ends of the whiskers), excluding outliers and extremes. Outliers are represented by the unfilled circles. Two outliers are noticed in Exp-2 and Exp-3 lying between 2 to 3 times the Inter-Quartile Range (IQR) from the edge of the respective box. From Fig. 13 it is clear that amongst the four experiments, the IQR is larger in Exp-4 with its value equal to 0.5 as against that in Exp-2 which is 0.4. Thus in Exp-4 and Exp-2, IQRs are close to the observed value which stands at 0.9. The medians in JJAS rainfall simulated in Exp-2 and Exp-4 are equal at 7.6mm/day as against the corresponding value of 7.55mm/day in case of IMD observed values. These two nearly equal numbers suggest that the experiments in which observed snow have been used as initial conditions, outperform the other two in which climatological snow are provided.

The IQRs of JJAS rainfall simulated in Exp-1 and Exp-3 are 0.2 and 0.25 respectively while their spreads range from 6.35 (mm/day) to 6.8 (mm/day) and from 6.2 (mm/day) to 6.9 (mm/day) respectively. The spread in case of Exp-2 (excluding the outliers), ranges from 6.95 (mm/day) to 8.25 (mm/day) and that based on Exp-4 rainfall ranges from 7.15 (mm/day) to 8.6 (mm/day). It is seen that the spread based on IMD observed rainfall lies between 6.1 (mm/day) to 8.9 (mm/day). These numbers give potentially useful information on the ranges of uncertainty in the rainfall simulated in all the four experiments as against those based on actually recorded rainfall by IMD. If we compare the four box-and-whiskers obtained based on the four experimental results with that in case of IMD recorded rainfall, then it is clear that those in Exp-2 and Exp-4 are closer to the IMD one as compared to the remaining two. Since observed SST and snow are used in Exp-2 and Exp-4 respectively, these results reconfirm the important role of observed SST and snow in simulating ISMR closer to the observed value. If we give a closer look to the characteristics of the box-and-whiskers based on Exp-2 and Exp-4 simulated rainfall and the IMD observed rainfall, we notice that the medians are same at 7.5, IQRs are 0.4, 0.5 and 0.9 respectively and the spreads are 1.3, 1.4 and 2.8 respectively. Thus the characteristics of box-and-whiskers obtained in Exp-4 are closer to those in IMD data as compared to Exp-2. Hence one can infer that Exp-4 has simulated ISMR closer to IMD observed values as compared to that in case of Exp-2.

Fig. 14 clearly brings out the relative importance of observed SST and snow in the context of JJAS rainfall simulation. In this figure, the first bar from the left indicates the difference between Exp-2 and Exp-1 in
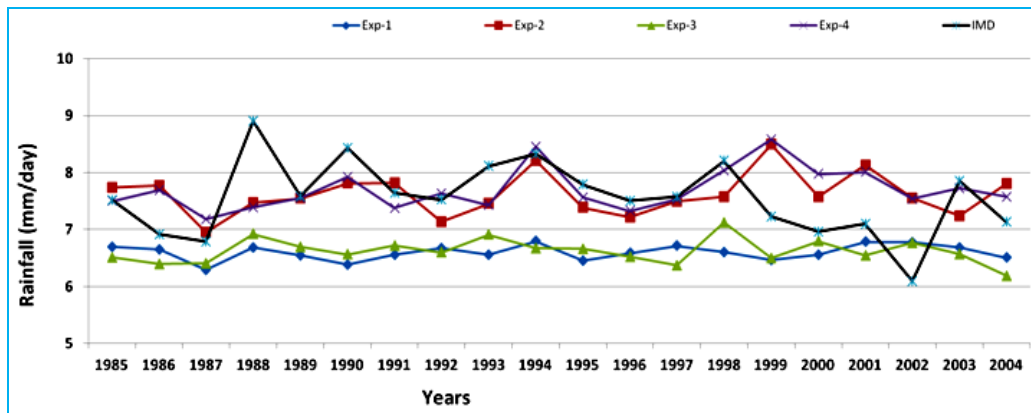
Fig. 11. Interannual variations in JJAS rainfall as simulated in the four experiments and reported by IMD
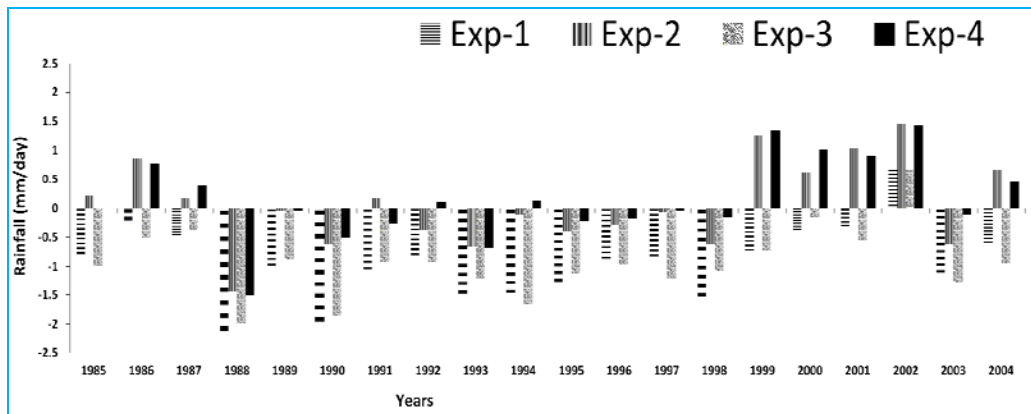
Fig. 12. Interannual rainfall differences (Exp-IMD) in all the four experiments
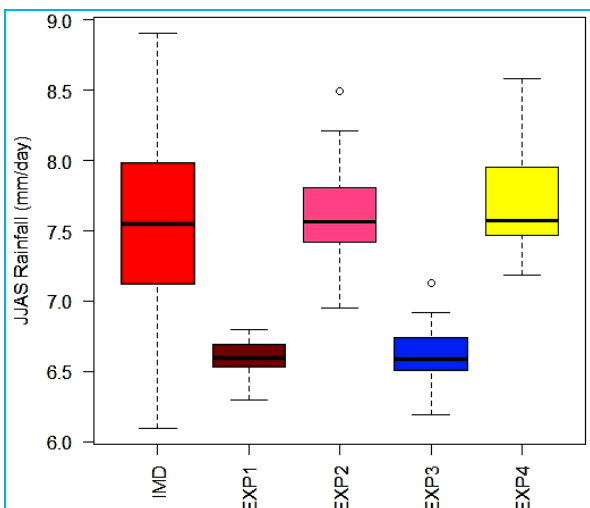
Fig. 13. Box plots representing IMD rainfall and the rainfall simulated by the model in all the four experiments. In the box plots, the bottom and top of each box indicate the 25th and 75th percentiles (the lower and upper quartiles) respectively and the band near the middle of a box is always the 50th percentile (the median). The outliers are denoted by 'o'

which climatological SST is the common factor in the surface boundary conditions. The only difference between Exp-2 and Exp-1 is the prescription of observed snow in Exp-2 and climatological snow in Exp-1. The change in ISMR by 1mm/day has happened due to the replacement of climatological initial snow values by the observed snow values, *i.e.*, due to snow anomaly in the presence of climatological SST. In the second bar, the common surface boundary condition to both Exp-3 and Exp-4 is the observed SST. As in case of the first bar, here the change of 1.2 mm/day in ISMR is due to the snow anomaly (replacement of climatological snow values by the respective observed values) but in the presence of observed SST. Thus one can attribute the change of 0.2 mm/day in ISMR from the first to the second bar to the combined effect of snow and SST anomalies (observed-climatology).

The third and fourth bars in Fig. 14 can be interpreted in an analogous manner. The third bar is obtained when the climatological snow is common to Exp-3 and Exp-1. Thus, the use of SST anomaly in the
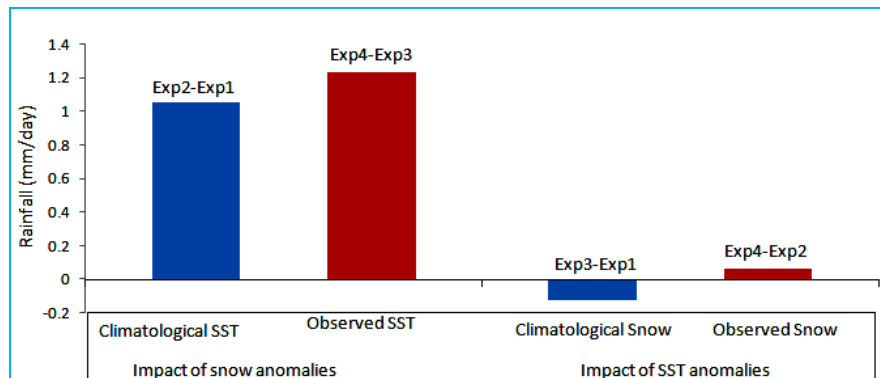
Fig. 14. Relative roles of climatological and observed SST and snow in simulating JJAS mean rainfall

presence of climatological snow has changed ISMR by about -0.17 mm/day. The decrease in ISMR in this bar can be explained by considering the facts that increase/decrease in ISMR depends on the type (negative/positive) of anomalies in SSTs and snow and also on their location. Here, the change from one bar to the other is considered as the impact of changes in snow and SST. The fourth bar is obtained due to SST anomaly when the observed snow is common in Exp-2 and Exp-4 and there is increase in the ISMR by 0.05 mm/day. Hence, the ISMR change of 0.22 mm/day from the third to the fourth bar suggests the additional role of snow anomaly in the presence of SST anomaly. Since the magnitudes of first two bars are much higher than those of the other two, it is clear that the snow anomaly either in the presence of climatological or observed SST as surface boundary conditions, has larger impact on the simulated ISMR as compared to that of SST anomaly in the presence of climatological/observed snow. Since we are examining the differences in ISMR, these results do not contradict the dominant role of SST as surface boundary condition in simulating ISMR. In fact, the first two bars happen in the presence of climatological/observed SST only.

Comparison of the difference between the first two bars in Fig. 14 clearly brings out the fact that the model simulated ISMR changes by 0.2 mm/day due to the combined effect of SST and snow anomalies. Nearly similar change of 0.22 mm/day change in ISMR occurs due to the combined impact of snow and SST anomalies as evident from the change from the third bar to the fourth. In other words, the change in ISMR due to the use of both realistic SST and snow is nearly the same whether one estimates the difference between the first two bars or the other two.

Thus, the model response to SST and snow anomalies in terms of simulated ISMR from the four experiments are consistent with each other. Further, these results reiterate the well known fact that the use of

observed SST and snow in model integrations is more realistic compared to the use of their climatological values.

7. Conclusions

The objective of this study is to examine the relative roles of SST and snow depth anomalies in simulating the Indian summer monsoon circulation and associated rainfall anomalies in a GCM. Both climatological and observed values of snow depth and SST are used in the model as surface boundary conditions. In this study the IITD spectral GCM at T80L18 resolution has been integrated in the ensemble mode for a period of 20 years from 1985 to 2004 to generate daily climatic fields. Eleven member ensemble seasonal integrations have been conducted from initial conditions of 25th April to 5th May for a period of 20 years from 1985 to 2004. The model is integrated up to the end of September with daily-observed SST and snow depth values. Four types of sensitive experiments have been conducted by varying the observed and climatological values of SST and snow for the whole period of model integration with a view to establish the important role of variation in snow depth in the summer monsoon simulation. In Exp-1, climatological SST and snow are prescribed in the model. Climatological snow depths are replaced by their corresponding observed values in Exp-2. Exp-3 is based on the observed SST and climatological snow. Finally, both observed SST and snow are used in Exp-4.

After a close examination of the model results, it is inferred that the use of observed snow in the model as initial condition plays a significant role in simulating the lower and upper level monsoon circulations and ISMR. The simulated wind characteristics at both the lower and upper levels in the atmosphere are close to their observed counterparts when observed snow depths are prescribed to the model as initial conditions in addition to the observed SST. The stream function and velocity potential fields confer to the same fact. More or less, the precipitation in

case of observed snow in Exp-2 and Exp-4 brings out the JJAS rainfall closer to the observed rainfall (IMD, Aphrodite and CRU) in central India. Thus the use of observed snow as initial condition in the model simulates the monsoon circulation and seasonal summer monsoon rainfall over central India well. Model simulated ISMR is found to agree with observation in 14 years out of 20 years of study. In the box-and whisker plots of rainfall, the spread in Exp-4 ranges from 7.15 (mm/day) to 8.6 (mm/day) and in Exp-2 it ranges from 7.05 (mm/day) to 8.25 (mm/day). In both these experiments, observed snow depths are prescribed to the model. The corresponding spread in IMD rainfall ranges from 6.1 (mm/day) to 8.9 (mm/day). These plots potentially give very useful information on the range of uncertainty. If we give a closer look to Exp-2 and Exp-4, we notice that with closer IQR of 0.5 and larger spread of 1.45, Exp-4 performs better against IMD values as compared to Exp-2. Results of this ensemble model integrations indicate that the model response in terms of ISMR anomalies to the snow anomalies in the presence of climatological SST is more than that of SST anomalies in the presence of climatological snow. Further, observed initial snow depths in the presence of observed SST, enhance the closeness of the model simulated Indian summer monsoon circulation and associated rainfall to the respective observed values.

References

Bamzai, A. S. and Shukla, J., 1999, "Relation between Eurasian snow cover, SD and the Indian summer monsoon: An observational study", *Journal of Climate*, **12**, 3117-3132.

Barnett, T. P., Dumenil, L., Schlese, U., Roeckner, E. and Latif, M., 1989, "The effect of Eurasian snow over on regional and global climate variations", *Journal of the Atmospheric Sciences*, **46**, 661-685.

Behera, S. K. and Yamagata, T., 2001, "Subtropical SST dipole events in the southern Indian Ocean", *Geophysical Research Letters*, **28**, 327-330.

Brankovic, C. T. N. and Palmer, 2000, "Seasonal skill and predictability of ECMWF PROVOST ensembles", *Quarterly Journal of the Royal Meteorological Society*, **126**, 2035-2068.

Charney, J. G. and Shukla, J., 1981, "Predictability of monsoons", *Monsoon Dynamics*, J. Light hill and R. P. Pearce, Eds., Cambridge University Press, 99-109.

Cherchi, A. and Navarra, A., 2003, "Reproducibility and predictability of the Asian summer monsoon in the Echam4 GCM", *Climate Dynamics*, **20**, 365-379.

Clark, C. O., Oelfke, C. J., Cole, J. E. and Webster, P. J., 2000, "Indian Ocean SST and Indian summer rainfall: Predictive relationships and their decadal variability", *J. Clim.*, **13**, 2503-2519.

Dash, S. K. and Chakrapani, B., 1989, "Simulation of a winter circulation over India using aglobal spectral model", *Proceedings of the Indian Academy of Sciences (Earth Planet Science)*, Section **98**, 189-205.

Dash, S. K. and Mohandas, S., 2005, "Comparative study of different orographic representations with respect to the Indian summer monsoon simulation", *Acta Geophysica Polonica*, **53**, 3, 325-340.

Dash, S. K., Parth Sarthi, P. and Panda, S. K., 2006, "A study on the effect of Eurasian snowon the summer monsoon circulation andrainfall using a spectral GCM", *Int. J. Climatol.*, **26**, 1017-1025.

Dash, S. K., Singh, G. P., Shekhar, M. S. and Vernekar, A. D., 2003, "Influence of Eurasian snow depth anomaly on the Indian summer monsoon circulation", *Mausam*, **54**, 2, 427-442.

Dash, S. K., Singh, G. P., Shekhar, M. S. and Vernekar, A. D., 2005, "Response of the Indian summer monsoon circulation and rainfall to seasonal snow depth anomaly over Eurasia", *Climate Dynamics*, **24**, 1-10.

Goswami, B. N. and Ajaya Mohan, R. S., 2001, "Intra-seasonal oscillations and predictability of the Indian summer monsoon", *Proc. Ind. Natl. Sci. Aca.*, **67A**, 3, 369-383.

Hahn, D. J. and Shukla, J., 1976, "An apparent relation between Eurasian snow cover and Indian monsoon rainfall", *Journal of the Atmospheric Sciences*, **33**, 2461-2462.

Kalnay, E., M. Kanamitsu, R. Kistler, W. Collins, D. Deaven, L. Gandin, M. Iredell, S. Saha, G. White, J. Woollen, Y. Zhu, M. Chelliah, W. Ebisuzaki, W. Higgins, J. Janowiak, K. C. Mo, C. Ropelewski, J. Wang, A. Leetmaa, R. Reynolds, Jenne Roy and Dennis Joseph, 1996, "The NCEP/NCAR 40-Year Reanalysis Project", *Bulletin of the American Meteorological Society*, **77**, 3, 437-471.

Keshavamurthy, R. N., 1982, "Response of the Atmosphere to Sea Surface Temperature Anomalies over the Equatorial Pacific and Teleconnections of the Southern Oscillation", *J. Atmos. Sci.*, **39**, 1241-1259.

Kothawale, D. R., Munot, A. A. and Borgaonkar, H. P., 2008, "Temperature variability over the Indian Ocean and its relationship with Indian summer monsoon rainfall", *Theor. Appl. Climatol.*, **9**, 31-45.

Kripalani, R. H. and Kulkarni, A., 1999, "Climatology and variability of historical Soviet snowdepth data: some new perspectives in snow-Indian monsoon tele-connection", *Journal of the Atmospheric Sciences*, **15**, 475-489.

Krishnamurthy, V. and Shukla, J., 2000, "Intraseasonal and interannual variability of rainfall over India", *J. Climate*, **13**, 4366-4377.

Kumar Krishna, K., Rajagopalan, B. and Cane, M. A., 1999, "On the weakening relationship between the Indian monsoon and ENSO", *Science*, **287**, 2156-2159.

Rajeevan, M., Bhate, J., Kale, J. D. and Lal, B., 2005, "Development of a high resolution daily gridded rainfall data for the Indian region", *IMD Met Monograph*, **No. Climatology 22/2005**, p27.

Rajeevan, M., Pai, D. S. and Thapliyal, V., 2002, "Predictive relationships between Indian Ocean sea surface temperatures and Indian summer monsoon rainfall", *Mausam*, **53**, 337-348.

Rao, K. G. and Goswami, B. N., 1988, "Interannual variations of sea surface temperature over the Arabian Sea and the Indian monsoon: A new perspective", *Mon. Wea. Rev.*, **116**, 558-568.

Reynolds, R. W. and Smith, T. M., 1994, "Improved global sea surface temperature analyses using optimum interpolation", *Journal of Climate*, **7**, 929-948.

Saha, S. K., Halder, S., Kumar, K. K. and Goswami, B. N., 2011, "Pre-onset land surface processes and 'internal' interannual variabilities of the Indian summer monsoon", *Climate Dynamics*, **36**, 11-12, 2077-2089.

Sankar-Rao, M., Lau, M. K. and Yang, S., 1996, "On the relationship between Eurasian snow cover and the Asian summer monsoon", *International Journal of Climatology*, **16**, 605-616.

Shukla, J., 1975, "Effect of Arabian sea-surface temperature anomaly on Indian summer monsoon: A numerical experiment with the GFDL model", *J. Atmos. Sci.*, **32**, 503-511.

Sikka, D. R., 1980, "Some aspects of the large-scale fluctuations of summer monsoon rainfall over India in relation to fluctuations in the planetary and regional scale circulation parameters", *Proc. Indian Acad. Sci. (Earth & Planet. Sci.)*, **89**, 179-195.

Sperber, K. R. and Palmer, T. N., 1996, "Interannual tropical rainfall variability in general circulation model simulations associated with the atmospheric model intercomparison project", *Journal of Climate*, **9**, 2727-2750.

Sperber, K. R., C. Brankovic, M. Deque, C.S. Frederiksen, R. Graham, A. Kitoh, C. Kobayashi, T. Palmer, K. Puri, W. Tennant and E. Volodin, 2001, "Dynamical seasonal predictability of the Asian summer monsoon", *Mon. Weather Rev.*, **129**, 2226-2248.

Turner, A. G. and Slingo, J. M., 2010, "Using idealized snow forcing to test teleconnections with the Indian summer monsoon in the Hadley Centre GCM", *Climate Dynamics*, **36**, 9-10, 1717-1735, DOI 10.1007/s00382-010-0805-3.

Vernekar, A. D., Zhou, J. and Shukla, J., 1995, "The effect of Eurasian snow cover on the Indian monsoon", *J. Climate*, **8**, 248-266.

Wang, X., Li, C. and Zhou, W., 2006, "Interdecadal variation of the relationship between Indian rainfall and SSTA modes in the Indian Ocean", *International Journal of Climatology*, **26**, 5, 595-606.